Drying of Ceramic Hollow Bricks in an Industrial Tunnel Dryer: A Finite Volume Analysis

Francisca Valdeiza de Souza Tavares [1,a], Severino Rodrigues de Farias Neto[2,a], Enivaldo Santos Barbosa[1,b], Antonio Gilson Barbosa de Lima[1,c*], Carlota Joaquina e Silva[1,d]

[1]Department of Mechanical Engineering, Federal University of Campina Grande (UFCG), Zip Code 58429-900, Campina Grande-PB, Brazil
[2]Department of Chemical Engineering, Federal University of Campina Grande (UFCG), Zip Code 58429-900, Campina Grande-PB, Brazil
[1c*]E-mail: gilson@dem.ufcg.edu.br
[1a]E-mail: valdeiza.tavares@hotmail.com
[1b]E-mail: enivaldo@dem.ufcg.edu.br
[1d]E-mail: carlotajs@gmail.com
[2]E-mail: fariasn@deq.ufcg.edu.br

ABSTRACT

This paper aims to study the drying of industrial hollow bricks in a tunnel dryer cross flow type. The theoretical model is based on mass and energy conservation equations applied to air and product. To validate the methodology, numerical and experimental results for the moisture content and the temperature of brick during the drying in an industrial scale are compared and a good correlation was obtained. Results of moisture content and temperature of the product, and temperature, relative humidity and absolute humidity of drying air as a function of drying time and position in the dryer are presented and analyzed.

Keywords: Simulation, Mass, Heat, Brick, Drying

1. INTRODUCTION

Ceramic processing has been studied based on the material formulation and industrial arts used in the production of commercial products. These products are very different in size, shape, detail, complexity, material composition, structure, and cost. In the manufacturing process of buildings bricks water is added to the clay before forming to increase plasticity.

Clay bricks are widely used by building industry and its manufacturing process includes several stages: exploration and pretreatment of raw materials, mixing with water, drying and firing. Drying is a thermodynamic process of fundamental importance in the manufacture of ceramic products, consisting in loss of water of the product by evaporation [1]. The drying can be explained also as a process of heat and mass transfer consisting in removing of the moisture contained within the product by evaporation at the surface of the solid [2]. After plastic forming and casting, brick must be dried, in order, to removal of the moisture prior for further processing and/or firing. If this moisture content is not removed adequately, severe stresses occurs inside the brick causing cracking and fissures reducing quality of product post-drying process. Then, the quality of the final product is directly related for this stage of the production process. Since for each product variations in the conditions of the

drying air affect the drying, so, the best drying parameters must be choice for obtain a smaller process time and better quality of product.

The convective drying technique differs from other separation techniques by the way as the water is removed from the solid. During the drying there is a difference in partial pressure of water vapor between the product surface and the air surrounding it, which gives the migration of the liquid inside out and hence the removal of the water molecules thereof.

During the process of drying the solids undergo variations in their chemical, physical and geometrical characteristics and depending on the intensity of the effect produced on the product, can cause the loss or make it inappropriate for certain functions [3].

The complexity of the drying process depends among other parameters on the thickness of the material layer. We can then classify them into thin-layer models (very fine layer of the material) and thick-layer models (dryer models). Of the practical viewpoint, thin-layer drying is very limited. But for have a good understanding of the drying process in thick layer it is necessary to have equations for the drying kinetics of a particular material in thin layer under certain predetermined operating conditions [4].

The drying of ceramics bricks can be made of natural or artificial manner. The process time depends on the especially conditions of the drying environment, such as temperature, relative humidity and velocity of the air and characteristics of the product. The technique of artificial drying has been widely used, as it significantly reduces the drying time. There is different type of dryers. One of the most currently used by the industrial sector is the tunnel dryer which is basically builded with metal or bricks. There is yet a rail in which moves a series of trolleys inside the dryer transporting the material to be dried.

Given the importance of the drying process a large number of researchers have devoted work on the drying analysis, with focus on the air external conditions such as temperature, relative humidity and velocity, correlated to the drying rate. Others consider the product internal conditions with emphasis on the mechanisms of moisture movement and its effects on the product quality. Knowledge of the mechanisms of water movement inside the materials is of fundamental importance and precedes the attempt to describe the migration of water in the mass of product [5].

Aiming to contribute with the advance in the technological field of drying, this paper presents a numerical study of drying of ceramic hollow brick in cross flow tunnel dryer, with emphasis on the heat and mass transfer between the product and air, and the influence of drying parameters on the drying and heating rates of the product, and post-drying quality.

2. METHODOLOGY

2.1 MATHEMATICAL MODELING

This work is based in one tunnel dryer with two fans that assist in directing the drying air to the product. The dryer receives the drying air reused of the kiln, with fixed temperature and relative humidity that arriving to the product by internal channels and are directed from bottom to top up as shown in Figure 1.

The bricks have geometrical shape of a parallelepiped and are transported in trolleys through rails, driven by piston. The drying is controlled basically through the moisture content of the product (Figure 2).

Mathematical modeling is based on the mass and energy balances for both the air and the product. Figure 3 shows a schematic view of product layer inside the dryer and an infinitesimal volume of this layer. It was assumed that the air velocity profile is plug type along the bed.

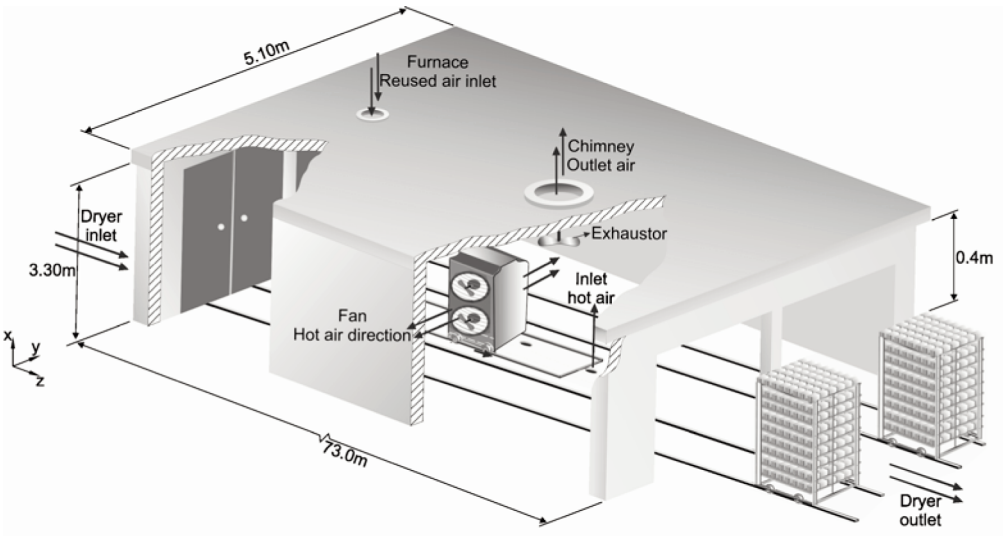

Figure 1: Schematic view and dimensions of the industrial dryer used in this work

The following equations are used:

- Energy balance for the air

$$\frac{\partial T}{\partial t}+\left(\frac{w}{\varepsilon}\right)\frac{\partial T}{\partial y}=-\frac{A^{*}h_{c}\left(T-\bar{\theta}\right)}{\varepsilon\left(\rho_{a}c_{a}+\rho_{a}\tilde{x}c_{v}\right)} \tag{1}$$

- Energy balance for the product

$$\frac{\partial\bar{\theta}}{\partial t}=\frac{A^{*}h_{c}\left(T-\bar{\theta}\right)}{\left(\rho_{p}c_{P}+\rho_{p}c_{W}\overline{M}\right)}+\frac{\left[h^{*}_{fg}+c_{v}\left(T-\bar{\theta}\right)\right]}{\left(\rho_{p}c_{P}+\rho_{p}c_{W}\overline{M}\right)}\rho_{p}\frac{\partial\overline{M}}{\partial t} \tag{2}$$

- Mass balance for air

$$\frac{\partial}{\partial t}\left(\rho_{a}\tilde{x}\right)+\nabla\left(\rho_{a}\frac{W}{\varepsilon}\tilde{x}\right)=-\frac{\rho_{p}}{\varepsilon}\frac{\partial\overline{M}}{\partial t} \tag{3}$$

- Mass balance of product [1]

$$\frac{\overline{M}-M_{e}}{M_{o}-M_{e}}=c_{1}\exp\left(k_{1}t\right)+c_{2}\exp\left(k_{2}t\right) \tag{4}$$

Differentiating Equation 4 we get:

$$\frac{\partial\overline{M}}{\partial t}=\left[c_{1}k_{1}\exp\left(k_{1}t\right)+c_{2}k_{2}\exp\left(k_{2}t\right)\right]\left(M_{0}-M_{e}\right) \tag{5}$$

where t is the time. The parameters c_1, c_2, k_1 and k_2 in Equation 5 were obtained by fitting to experimental data of moisture content by [1]. Table 1 shows the values of these parameters. In the Equations 1, 2 and 3, $\tilde{x}$, T and w represent absolute humidity, temperature and velocity of the air respectively, and $\bar{\theta}$ and M represent temperature and moisture content of the product respectively. ε is the bed porosity.

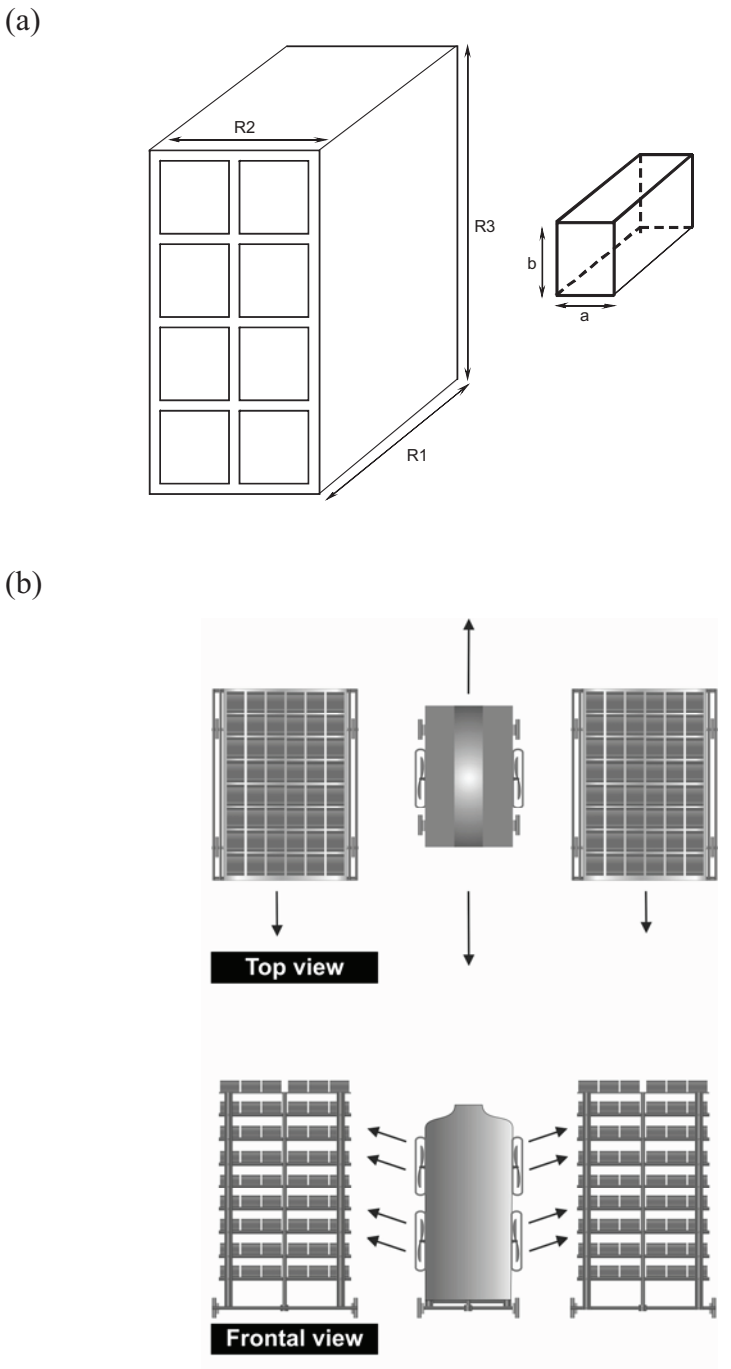

Figure 2: (a) Brick used in the drying process (b) View of the trolley fan and air flow

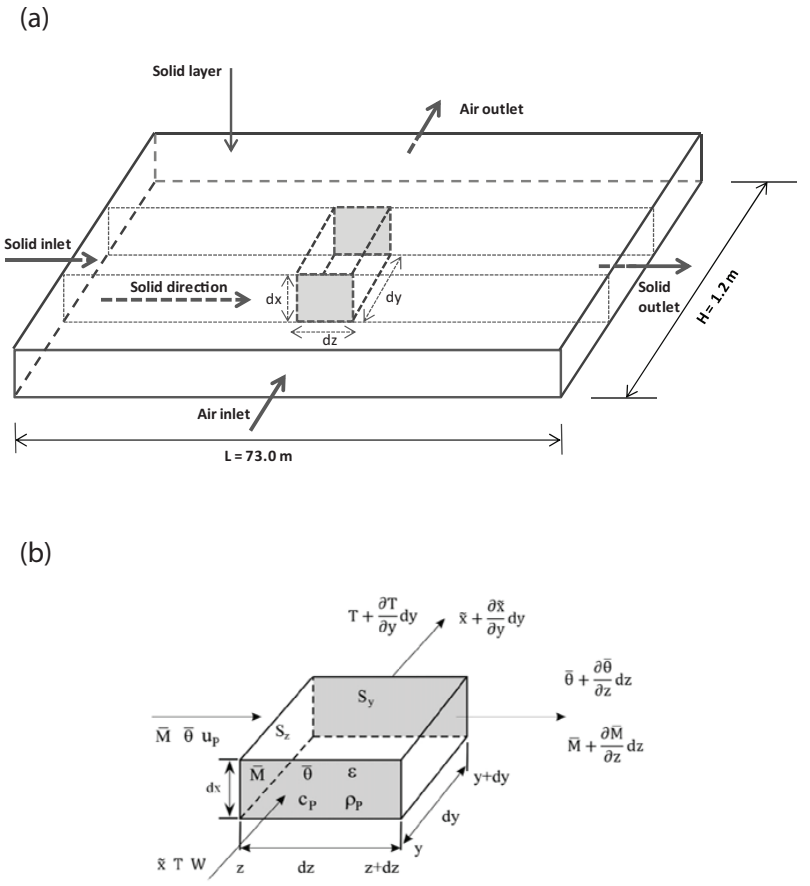

Figure 3: Schematic view of a (a) porous solid layer inside the of cross flow tunnel dryer and (b) infinitesimal volume of the solid layer

Table 1: Parameters of the drying rate equation for three temperatures

T(°C)	Parameters					
	c_1	k_1	c_2	k_2	M_o (kg/kg)	M_e (kg/kg)
50	0.576178	–0.0047115	0.4822324	–0.0047112	0.13969	0.00011
60	0.54774	–0.0059453	0.5133493	–0.0059452	0.14795	0.00268
70	-1.083353×10^{-18}	0.0067809	1.04505	–0.0070948	0.15414	0.00076

In this research the dryer was divided into three sections. The initial and boundary conditions are shown schematically in Figure 4 and cited following:

$\overline{M}(y,z=0,t=0)=\overline{M}_o$ $\quad$ $\overline{\theta}(y,z=0,t=0)=\overline{\theta}_o$

$T(y=0, z<L/3, t)=T_1$ $\quad$ $\tilde{x}(y=0, z<L/3, t)=\tilde{x}_1$

$T(y=0, L/3\le z<L/1.5, t)=T_2$ $\quad$ $\tilde{x}(y=0, L/3\le z<L/1.5, t)=\tilde{x}_2$

$T(y=0, L/1.5\le z<L, t)=T_3$ $\quad$ $\tilde{x}(y=0, L/1.5\le z<L, t)=\tilde{x}_3$

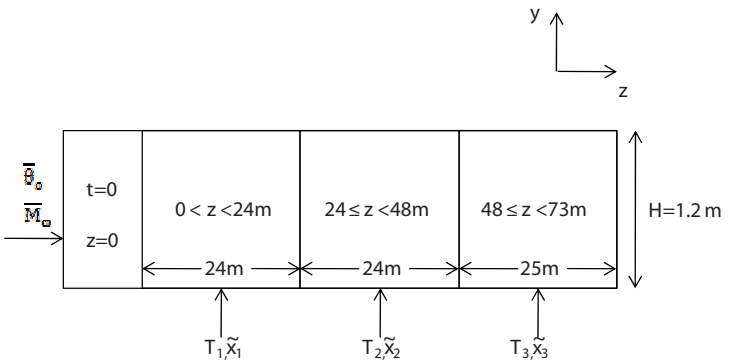

Figure 4: Scheme of the initial and boundary conditions in the dryer

The latent heat of vaporization of water, specific heat of brick, density of dry solid, product volume, surface area of contact, specific surface area and volume fraction of the bed (porosity) are defined by [6].

$$h_{fg} = 352.8\ (374.14\text{-}T)^{0.33052} \tag{6}$$

$$c_P = 1.673 \times 10^3\ \text{J/kgK}$$

$$\rho_P = 1985.8\ \text{kg/m}^3$$

$$V_P = 0.00131\ \text{m}^3$$

$$\varepsilon = 0.864401$$

$$A_P = 0.3332\ \text{m}^2$$

$$A^* = \frac{A_P(1-\varepsilon)}{V_P} \tag{7}$$

The specific heat of air, air density, absolute temperature, universal constant of air, relative humidity, saturated vapor pressure, and local atmospheric pressure, are determined by [7, 8].

$$c_a = 1.00926 - 4.04033 \times 10^{-5} T_a + 6.17596 \times 10^{-7} T_a^2 - 4.0972 \times 10^{-10} T_a^3\ \text{(kJ/kgK)} \tag{8}$$

$$\rho_a = \frac{P_{atm} M_a}{R T_{abs}}\ (\text{kg/m}^3) \tag{9}$$

$$T_{abs} = T_a + 273.15\text{K} \tag{10}$$

$$R_a = 8314.34\ \text{J/kg}\ ^{\circ}\text{C}$$

$$RH = \frac{P_{atm} \tilde{x}_a}{(\tilde{x}_a + 0.622) P_{vs}} \tag{11}$$

$$P_{vs} = 22105649.25\ \text{Exp}\ \{[-27405.53 + 97.5413 T_{abs} - 0.146244 T_{abs}^2 + 0.12558 \times 10^{-3}\ T_{abs}^3 - 0.48502 \times 10^{-7}\ T_{abs}^4]/[4.34903 T_{abs} - 0.39381 \times 10^{-2}\ T_{abs}^2]\}\ (\text{Pa}) \tag{12}$$

$$P_{atm} = 101325\ \text{Pa}$$

The specific heats of water in liquid and vapor phases are calculated as follows:

$$c_w = 2.82232 + 1.18277 \times 10^{-2} T_{abs} - 3.5047 \times 10^{-5} T_{abs}^2 + 3.6010 \times 10^{-8} T_{abs}^3\ \text{(kJ/kgK)} \tag{13}$$

$$c_v = 1.8830 - 0.16737 \times 10^{-3} T_{abs} + 0.84386 \times 10^{-6} T_{abs}^2 - 0.26966 \times 10^{-9} T_{abs}^3\ \text{(kJ/kgK)} \tag{14}$$

To calculate the convective heat transfer coefficient, we used the equation reported by [9]. The Equation 15 can be used for non-circular duct of rectangular shape, similar to geometry of the brick.

$$h_c = (k_a/D_h)(0.023 Re^{4/5} Pr^{1/3}) \tag{15}$$

where,

$D_h = 2ab/(a+b)$ is the hydraulic diameter of the brick with rectangular ducts and a and b are the dimensions of the rectangular section of the hole in the brick.

$$Re = \frac{\rho_a w_a R_1}{\mu_a} \text{ is the Reynolds number;} \tag{16}$$

$$Pr = \frac{c_a \mu_a}{k_a} \text{ is the Prandtl number;} \tag{17}$$

2.2 NUMERICAL SOLUTION

The solution the transient problem addressed in this study was obtained using the numerical method of finite volume [10, 11]. The Figure 5 illustrates a numerical scheme of the control volume considered in this work, where the nodal point P (including dimensions) and its neighboring S (south) and N (north) are highlighted.

After the integration of the partial differential equations on the volume and time, has resulted in a system of linear equations, in its discretized form as follows:

- Energy balance for air

$$A_P T_P = A_S T_S + A_P^o T_P^o + S_C^T \tag{18}$$

- Energy balance for the product

$$A_P \bar{\theta}_P = A_p^o \bar{\theta}_p^o + S_c^{\bar{\theta}} \tag{19}$$

- Mass balance air

$$A_P x_P = A_S x_S + A_p^o x_p^o + S_c^x \tag{20}$$

- Mass balance of product

$$A_P \bar{M}_P = A_p^o \bar{M}_p^o + S_c^{\bar{M}} \tag{21}$$

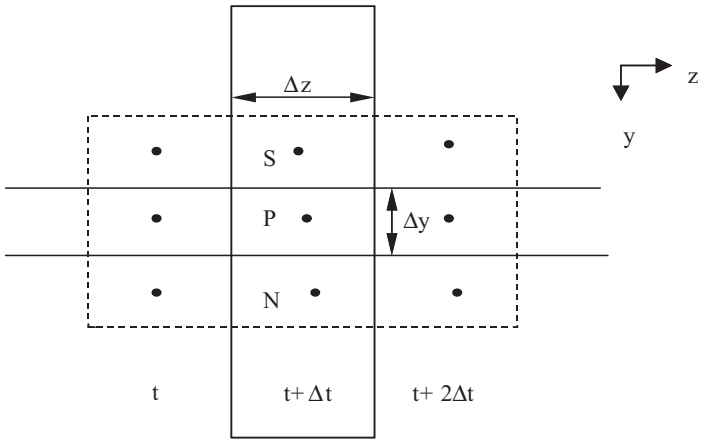

Figure 5: Numerical scheme and the control volume used in present work

Table 2: Parameters used in the simulation of drying of hollow ceramic bricks in a cross-flow tunnel dryer

Parameters	**Variable**	**Value**
Temperature of the drying air in section 1	T_1 (ºC)	50
Temperature of the drying air in section 2	T_2 (ºC)	60
Temperature of the drying air in section 3	T_3 (ºC)	70
Humidity ratio of air in section 1	$\tilde{x}_1$ (kg/kg)	0.01617
Humidity ratio of air in section 2	$\tilde{x}_2$ (kg/kg)	0.01697
Humidity ratio of air in section 3	$\tilde{x}_3$ (kg/kg)	0.0149
Speed of drying air	w_a (m/s)	20
Total length of the dryer	L (m)	73
Length of the brick layer	h (m)	2.86
Depth of the brick layer	H (m)	1.2
Initial temperature of product	θ_0 (°C)	20.5
Length of the brick	R_1 (mm)	200
Depth of the brick	R_2 (mm)	90
Height of the brick	R_3 (mm)	190
Speed of the trolley	u_p (m/s)	0.00088
Dimensions of the holes in the brick	a × b (mm)	34 × 40

In Equations 1 and 3 was used the upwind scheme as interpolation function for the convective terms and a parabolic procedure in the z direction [10]. Details about the coefficients A_p, A_k and S_c can be found in [12]. Table 2 provided the parameters used in the simulations. For obtain the results was developed a computational code in Mathematica® language and was used a mesh of 20 nodal points. It is noteworthy that the gradients of moisture and temperature of the product and absolute humidity and temperature of air occur in the directions of airflow and the dryer outlet. None change in the air and brick occurs in the direction perpendicular to the aforesaid directions. This is due the fact the dryer to be regarded as a single trolley given that the trolleys are introduced one by one by filling its entire length.

3. RESULTS AND DISCUSSION

To validate the methodology, were compared numerical results of the moisture content of the ceramic hollow brick with experimental data of the drying in oven reported in the literature [1]. This comparison is possible because the analysis considers only the first layer of bricks in the bed (y = 0) and low velocity of the trolley, which allows a better comparison and therefore a better approximation of the results. Figure 6 illustrates the experimental and numerical curves for the moisture content as a function of the time for the studied case. Figure 7 shows the behavior of the temperature along the process at the same location (y = 0). From the analysis of the Figure 6 can be observed that at the end of the first section of the dryer, which has a length of 24m, the product has almost reached the equilibrium moisture content. Regarding temperature (Figure 7) is worth noting that the comparison between numerical and experimental data is done only for the first section of the dryer, where the air entry conditions used in the numerical simulation and experiments are equal. The difference between the numerical and experimental data can be explained because the velocity of the drying-air which has been used in the simulation is higher than the air velocity inside the oven, which considerably increases the convective heat transfer coefficient at the surface of the brick, thus increasing heating rate. Further, it can also be attributed to the procedure used in the experiments such as the position of the brick inside the oven.

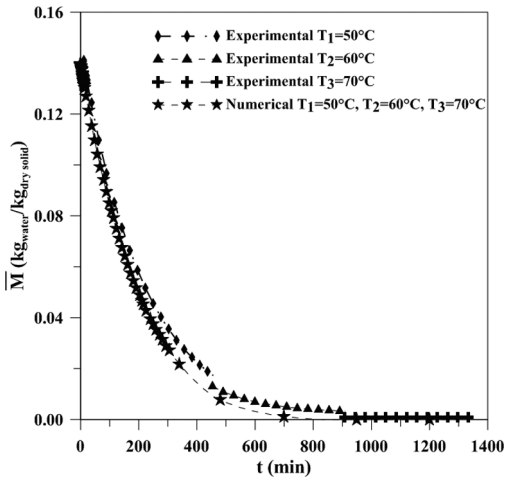

Figure 6: Comparison (y = 0) between predicted and experimental moisture content data of the brick [1] as a function of the drying time

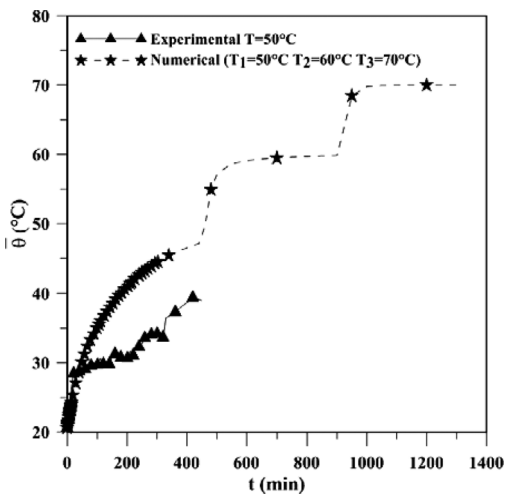

Figure 7: Comparison (y = 0) between predicted and experimental temperature of the brick [1] as a function of the drying time

Figures 8–11 show the behavior of the average moisture content of the brick ($\overline{M}$), product temperature ($\overline{\theta}$), air relative humidity (RH), air absolute humidity ($\tilde{x}$), and saturated vapor pressure (Pvs) as a function of the time, respectively, for the first (y = 0) and the last (y = H) layer.

It is possible to see that the first and last layer dries so as practically equal. This is due to the fact that the amount of moisture in the vapor phase that is transferred to the air in the beginning of the bed is not sufficient to decrease its potential of drying, thus the air can absorb moisture in the last layer almost the same amount of water absorbed in the first layer of the brick. This is an interesting point, because this air can be re-used, including drying.

By comparing the Figures 8 and 9 we can see that the brick temperature presents low value (50°C) when the product is almost dried (t = 6 h). Following the brick have increased

the temperature until reach the thermal equilibrium at the maximum air temperature on the third sector (70°C) in t = 24 h of the process. The increase in the temperature is soft, thus, we have a good control of this drying parameter related to brick quality.

Regarding the air relative humidity in the first layer (y = 0) (Fig. 10), we can see that practically this parameter does not vary. However, in the last layer (y = H) of the first section of the dryer shows a peak that decreases over time. Regarding the air absolute humidity (Figure 11) we note that in the last layer (y = H) of the first section there is a sudden increase, followed of a decreases along the process. These phenomena is because the air that reaches the last layer of the bed early in the process, has received a large amount of water in the vapor phase coming from the first layers of the bricks.

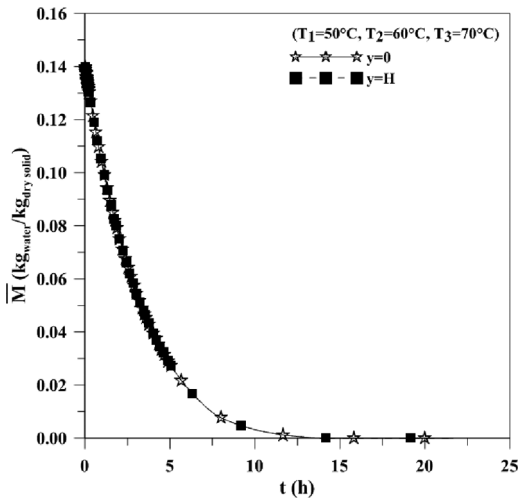

Figure 8: Data comparison of the moisture content of the brick at the first layer (y=0) and last layer (y=H) of the bed

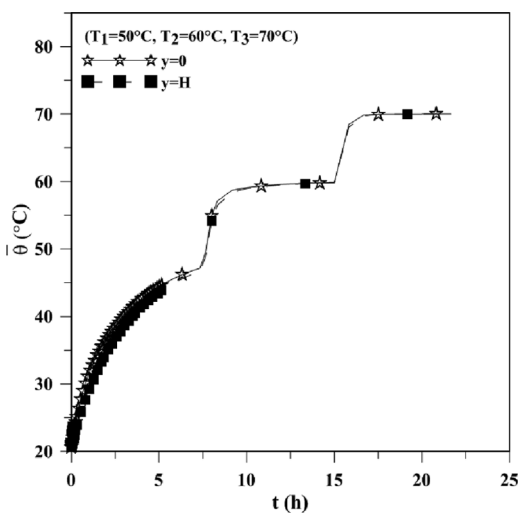

Figure 9: Data comparison of the product temperature at the first layer (y=0) and last layer (y=H) of the bed of product temperature

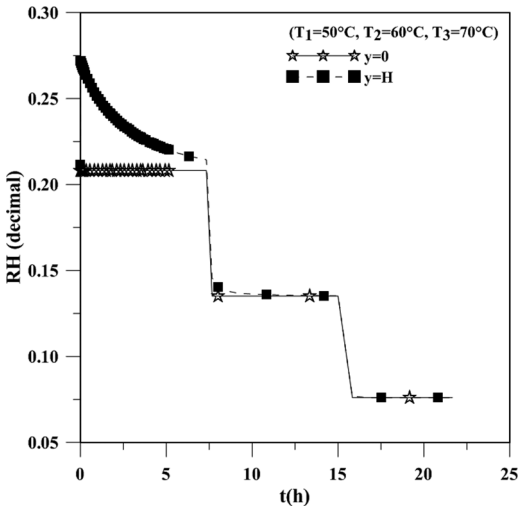

Figure 10: Data comparison of the air relative humidity in the first layer (y=0) and last layer (y = H) of the bed

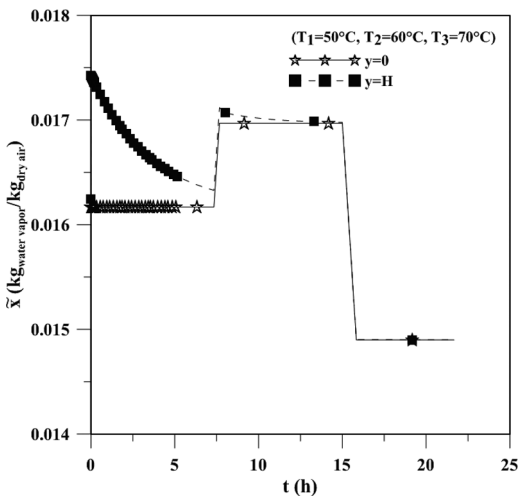

Figure 11: Data comparison of the air absolute humidity in the first layer (y=0) and last layer (y = H) of the bed

Figures 12–16 show the values of the moisture content ($\overline{M}$), product temperature ($\overline{\theta}$), drying air temperature (T), air relative humidity (RH), air absolute humidity ($\bar{x}$) at different times along the bed. From the analysis of the Figures 12 and 13 it is noted at the times preestablished that both moisture content and product temperature practically does not vary along the bed. Thus, there is not the presence of high hydro and thermal gradients in the brick layer during the drying process. This can be explained by the fact that the temperature of the drying air used in the simulation was gradually increased. Although the low relative humidity of the drying air. Similar behavior was verified to the air inside the bed along the drying process.

We notice that the temperature and relative humidity of the drying air have a strong influence on the kinetics of the process (heating and drying rates). In Figure 14 it is notable that

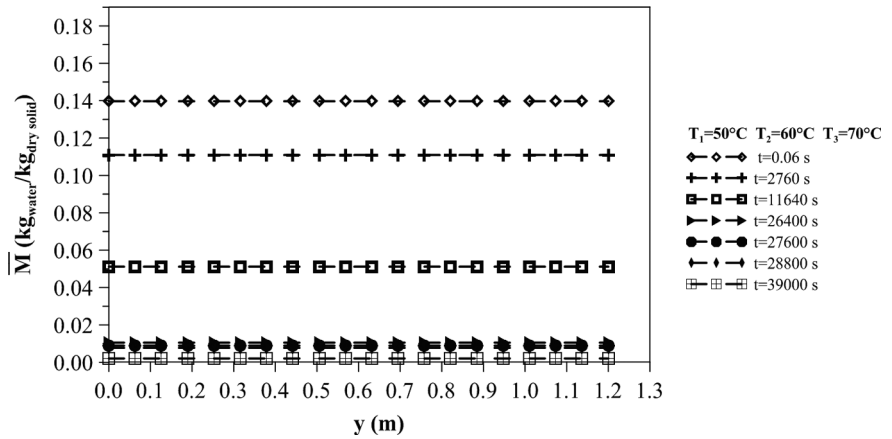

Figure 12: Predicted data of the brick moisture content in the bed at different times

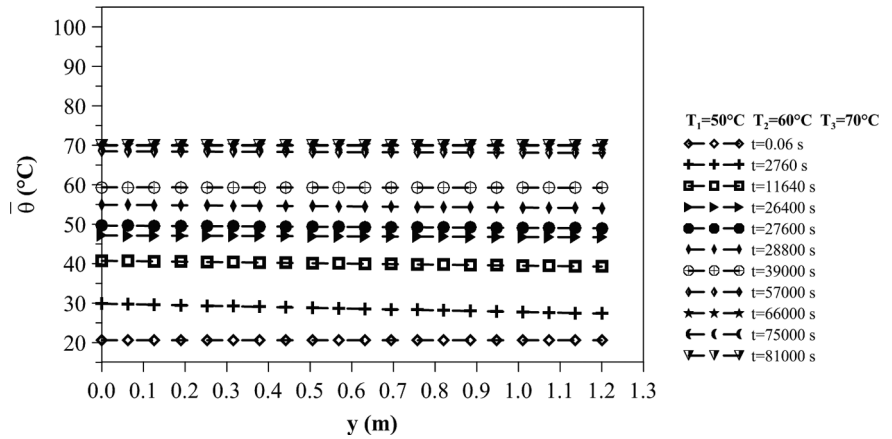

Figure 13: Predicted data of the brick temperature in the bed at different times

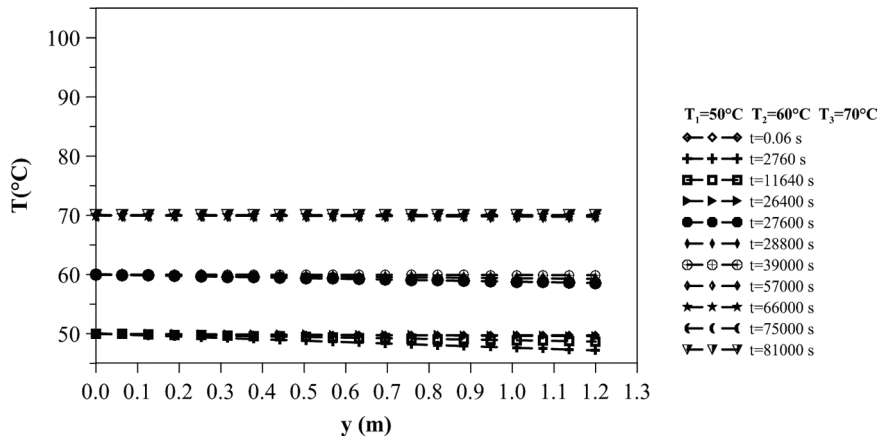

Figure 14: Predicted data of the air temperature in the bed at different times

early the air temperature decreases slightly (t = 2760s) at the end of the bed (y = H) and then goes back to grow. This is due of the fact that the air supply energy to the brick, thus decreasing its temperature. This convective energy is responsible to heat the product, evaporates the liquid water at the surface of the brick and to heat the vapor since the surface temperature until the drying air temperature. From the analysis of the Figures 15 and 16 show that the air is with great potential for drying, i.e., it is with low both relative humidity and absolute humidity.

The increase in temperature and decrease in relative humidity of the drying air increases both the drying and heating rates and the brick reaches more quickly the temperature and moisture balance. High thermal and moisture gradients within the brick and layer of the bed are not advisable because they produce non-uniform drying and great thermal, hydro and mechanical stresses inside the brick, which can cause cracks, fissures, and deformation in them. These stresses affect the brick quality at the end of the process and thus making unfeasible their marketing. It is of great importance prior to have control in drying. If drying is not uniform, certainly will appear distortions in pieces, on the other hand if it is too slow, the production process became uneconomical [13].

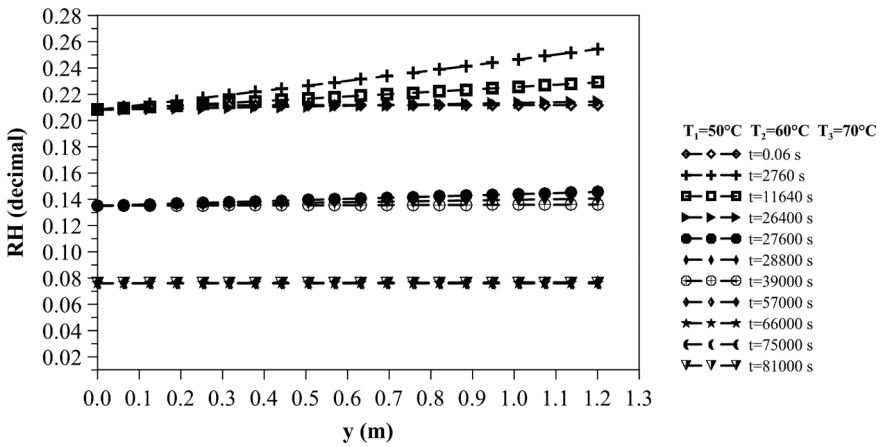

Figure 15: Predicted data of the air relative humidity in the bed at different times

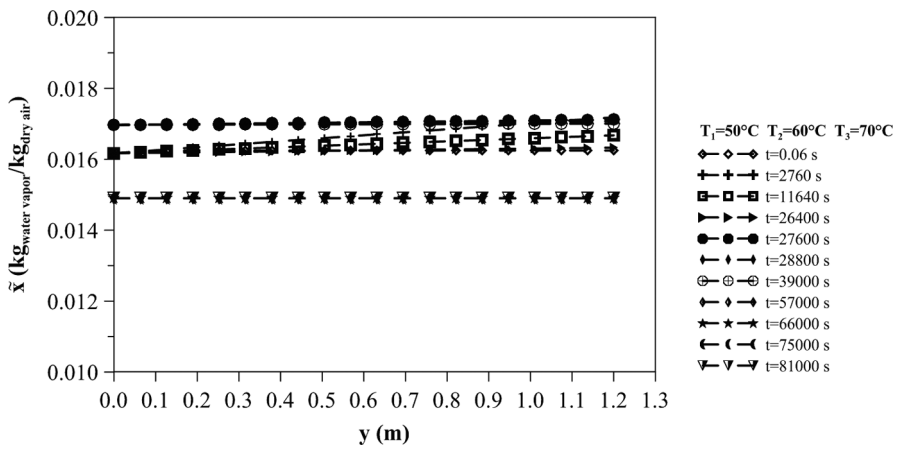

Figure 16: Predicted data of the air absolute humidity in the bed at different times

4. CONCLUSIONS

Based on the information presented in this paper, the following conclusions can be cited:

a) The mathematical model presented describes well the drying phenomena of hollow ceramic brick in cross flow tunnel dryer.

b) The finite-volume method was adequate to discretize the basic equations and numerical results showed good agreement with the experimental data of moisture content of bricks subjected to drying, thus showing that the methodology used is satisfactory.

c) The conditions of the drying-air have direct influence on the drying kinetics of the brick: high air temperature and lower air relative humidity imply that the material dry faster, and possibly reduces brick quality post-drying.

ACKNOWLEDGEMENTS

The authors thank to FINEP, CAPES, CNPq and FACEPE (Brazilian Research Agencies) for financial support to this research, and also to the researchers for their referenced studies which helped in improving the quality of this work.

REFERENCES

[1] J. B. Silva, Simulation and Experimentation of the Drying of Holed Ceramic Bricks. Thesis (Doctorate in Process Engineering), Federal University of Campina Grande, Campina Grande-Brazil, 2009. (In Portuguese).

[2] M. Fortes, M. R. Okos, Advances in Drying. Washington: Hemisphere Publishing Corporation, Chapter Five: Drying theories: their bases and limitations as applied to foods and grains, v.1, p. 119–154. 1980.

[3] V. A. B. Oliveira, Heat and Mass Transfer Inside the Solids with Prolate Spheroidal Shape via Thermodynamics of Irreversible Processes. Thesis (Doctorate in Process Engineering), Federal University of Campina Grande, Campina Grande-Brazil, 2006. (In Portuguese).

[4] R.P. Farias, Biological Products Drying Simulation in Crossflow Dryer. Dissertation (Master in Mechanical Engineering), Federal University of Campina Grande, Campina Grande-Brazil, 2003. (In Portuguese).

[5] P. R. H. Holanda, Dryer for Cocoons of the Silkworm*:* Development, Simulation and Experimentation. Thesis (Doctorate in Process Engineering), Federal University of Campina Grande, Campina Grande-Brazil, 2007, p. 161. (In Portuguese).

[6] Z. Pakowski, Z. Bartczak, C. Strumillo, S. Stenstrom, Evaluation of Equations Approximating Thermodynamic and Transport Properties of Water, Steam and Air for Use in CAD of Drying Processes, Drying Technology, v. 9 (1991) 753–773.

[7] R.Y. Jumah, A.S. Mujumdar, G.S.V.A. Raghavan, Mathematical Model for Constant and Intermittent Batch Drying of Grains in a Novel Rotating Jet Spouted Bed, Drying Technology 14 (1996) 765–802.

[8] S.J. Rossi, Psychrometry, FUNAPE, João Pessoa, Brazil, 1987. (In Portuguese).

[9] G. S. Almeida, Simulation and Experimentation of Red Ceramics Drying in Industrial Thermal Systems. Thesis (Doctorate in Process Engineering), Federal University of Campina Grande, Campina Grande-Brazil, 2009, p. 211. (In Portuguese).

[10] C.R. Maliska, Computational Heat Transfer and Fluid Mechanics, LTC-Livros Técnicos e Científicos Editora S.A, Rio de Janeiro, Brazil, 2004. (In Portuguese).

[11] S.V. Patankar, Numerical Heat Transfer and Fluid Flow, Hemisphere Publishing Corporation, New York, USA, 1980.

[12] G. S. Almeida, J. B. Silva, C. J. Silva, R. Swarnakar, G. A. Neves, A. G. B. Lima, Heat and Mass Transport in an Industrial Tunnel Dryer: Modeling and Simulation Applied to Hollow Bricks, Applied Thermal Engineering, 55, Issues 1–2 (2013) 78–86.

[13] J. J. S. Nascimento, Transient Phenomena of Diffusion in Solids Parallelepipeds. Case Study: Drying of Ceramic Materials. Thesis (Doctorate in Mechanical Engineering), Federal University of Paraiba, João Pessoa-Brazil, 2009. (In Portuguese).